Supporting Information

Pei et al. 10.1073/pnas.1012588108

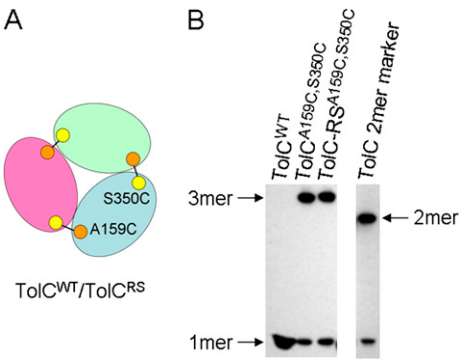

Fig. S1. Do asymmetric intermediates of the TolC entrance open state exist in vivo? We set out to establish whether intermediates characteristic of a purported asymmetric opening exist, and could be captured in vivo, reasoning that an asymmetric mechanism, in which protomers are suggested to act independently, would generate entrance dimers. To capture such purported intermediates, whether stable or transient, we established a means to isolate TolC protomers in dimeric, or trimeric, configuration by allowing interprotomer covalent links to form at the entrance. (*A*) Introducing "self-locking" disulfide bridges to capture purported intermediates in the opening mechanism. Cysteines were introduced at A^{159} and S^{350} on TolC H4/H7 (separated by 4.2 Å) just above the pore constriction (Fig. 1, cross-section 1) to allow interprotomer covalent linkage of TolC dimers and/or trimers via disulfide bridges. Cysteines were introduced by site-directed mutagenesis into $TolC^{WT}$ and the $TolC^{RS}$ initial open state (1). (*B*) Direct isolation of in vivo "self-locked" oligomers. Double cysteine variants of $TolC^{WT}$ ($TolC^{S350C,A159C}$) and $TolC^{RS}$ (TolC-$RS^{S350C,A159C}$) were grown in media containing the inhibitory drug novobiocin (50 μg/mL), an efflux substrate of the AcrA-AcrB-TolC drug efflux pump. Whole-cell proteins were analyzed by SDS/PAGE and immunoblotting with TolC antiserum. In both $TolC^{S350C,A159C}$ and TolC-$RS^{S350C,A159C}$ a mixture of monomers and trimers is evident, but in neither case are any dimers evident (migration of the dimeric configuration is indicated by the size marker homobifunctional bis-maleimidoethane (BMOE) cross-linked $TolC^{D374C}$; Fig. S3). Conclusion: The results reveal there was no capture of any dimer intermediates, stable or transient, that would be expected in an asymmetric peristaltic opening mechanism in which each protomer acts independently. The results are compatible with an opening mechanism in which all three protomers dilate in unison into a threefold symmetrical arrangement.

1. Eswaran J, Hughes C, Koronakis V (2003) Locking TolC entrance helices to prevent protein translocation by the bacterial type I export apparatus. *J Mol Biol* 327:309–315.

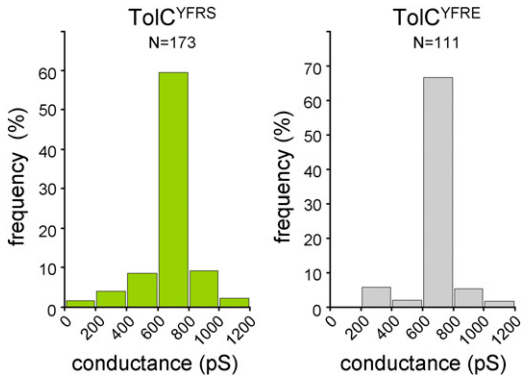

Fig. S2. Are intermediate "asymmetric" open states evident in TolC channel populations? We set out to measure the conductance of populations of channels formed by the symmetrical TolC^{YFRS} and the purportedly asymmetric TolC^{YFRE} in lipid bilayers. We reasoned that if the TolC^{YFRE} crystal structure obtained at high pH reflected a physiologically pertinent opening, the substantial difference in its pore constriction cross-sectional area compared with that of TolC^{YFRS} (26.4 Å^2 against 50.2 Å^2, calculated by HOLE, ref. 1) should determine a marked difference in channel conductances. In addition, the purported asymmetric opening could generate major intermediate conductances, which would be detectable in channel populations. Distribution of conductances of TolC^{YFRS} and TolC^{YFRE} channels in lipid bilayers. To do this, TolC^{YFRE} protein was created by site-directed mutagenesis and, like TolC^{YFRS}, it was expressed in TolC^{-} *E. coli* (3). Both proteins, TolC^{YFRE} and TolC^{YFRS}, were isolated from the bacterial membranes as described in the main text for TolC^{YFRS} crystallization. The electrophysiology methodology was essentially as we have described previously for TolC (2–5): proteins were added to artificial membranes formed by a 1% solution of diphytanoyl phosphatidylcholine and bathed in 1 M KCl, pH 7.5, i.e., physiological pH. The conductances of random populations of resulting channels, 173 of TolC^{YFRS} and 111 of TolC^{YFRS}, were measured at 20 mV. The frequency of the channel conductances is presented. Conclusion: The results show that the distribution of conductances in the two variants is essentially identical; there is a single major open state (conductance value) in both TolC^{YFRS} and TolC^{YFRE}, around 800 pS. There is no stable intermediate state evident in TolC^{YFRE}, and the TolC^{YFRE} channels are the same size as those of the closely analyzed, symmetrical TolC^{YFRS}. This is logical as their disrupted bonds are identical, apart from substitution of the positive Arg^{367} by negatively charged Glu in the TolC^{YFRE} entrance. The data provide no evidence of any additional stable major substates of opening stages that could be generated in a purported asymmetric opening mechanism. They show that the two variants, TolC^{YFRS} and TolC^{YFRE}, are essentially identical at physiological pH, supporting the view that the asymmetrical, smaller pore constriction of TolC^{YFRE}, visualized at pH 10.5, is a crystallographic artifact.

1. Smart OS, Goodfellow JM, Wallace BA (1993) The pore dimensions of gramicidin A. *Biophys J* 65:2455–2460.
2. Andersen C, et al. (2002) Transition to the open state of the TolC periplasmic tunnel entrance. *Proc Natl Acad Sci USA* 99:11103–11108.
3. Eswaran J, Hughes C, Koronakis V (2003) Locking TolC entrance helices to prevent protein translocation by the bacterial type I export apparatus. *J Mol Biol* 327:309–315.
4. Higgins MK, et al. (2004) Structure of the ligand-blocked periplasmic entrance of the bacterial multidrug efflux protein TolC. *J Mol Biol* 342:697–702.
5. Andersen C, Hughes C, Koronakis V (2002) Electrophysiological behavior of the TolC channel-tunnel in planar lipid bilayers. *J Membr Biol* 185:83–92.

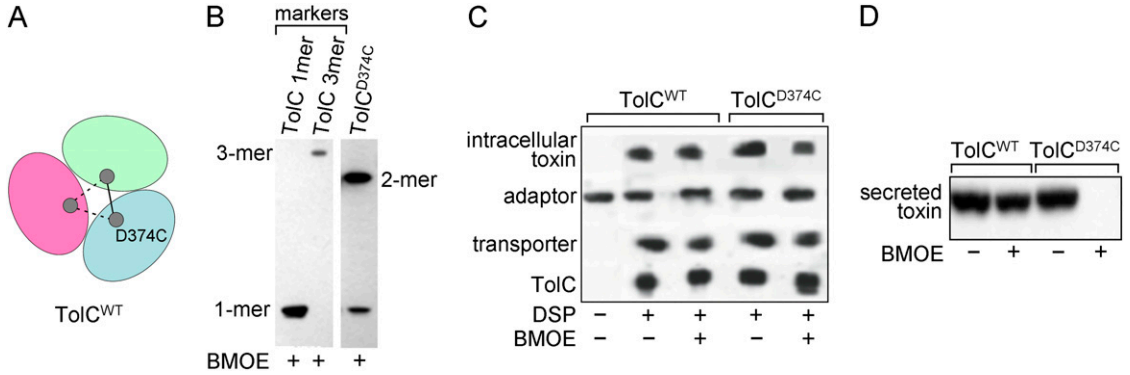

Fig. S3. Is a forced asymmetric TolC entrance functional in vivo? As we were unable to find any evidence of an asymmetric configuration of the TolC entrance, we set out to impose asymmetry, specifically on the pore constriction itself, and to assess whether this configuration was functional, i.e., allowed passage of substrate that is engaged in an assembled tripartite pump. To do this, we assayed function of the HlyB-HyD-TolC toxin export machinery, assembly of which we can follow in response to engagement by the export substrate, the protein toxin HlyA. (*A*) Forcing the TolC entrance pore constriction into an asymmetric configuration by chemical cross-linking. Cysteines were introduced by site-directed mutagenesis into the pore constriction at D^{374} (Fig. 1*B*, cross-section 1) of the naturally cysteine-free $TolC^{WT}$ to generate $TolC^{D374C}$ (1). The cysteine residues are 6.1 Å apart and therefore only form connections in the presence of the homobifunctional bis-maleimidoethane (BMOE), a cross-linker that has two sulfhydryl reactive groups and a spacer arm of 8 Å. BMOE therefore links C^{374} of adjacent protomers, i.e., covalently linking two of the three protomers (bold line) at any time, leaving one protomer free. This effectively forces the TolC entrance into an asymmetric state in vivo. (*B*) An asymmetric configuration of the $TolC^{D374C}$ pore constriction imposed by covalent cross-linking. $TolC^{D374C}$ was expressed in a $TolC^{-}$ *E. coli* strain as were $TolC^{WT}$ and $TolC^{A159C,S350C}$ (Fig. S1), which provide monomer and trimer markers. Cultures were treated with BMOE cross-linker as described in Eswaran et al. (1); proteins were separated by SDS/PAGE and analyzed by immunoblotting with TolC antiserum. The results show that $TolC^{D374C}$ forms only dimers and their concomitant monomers, which were not covalently linked by the cross-linker. It forms no trimers, confirming the asymmetric state is imposed in the presence of cross-linker. (*C*) Asymmetrically cross-linked $TolC^{D374C}$ assembles in vivo into the tripartite pump assembly of the type I tripartite export pump in *E. coli* expressing $TolC^{D374C}$ or $TolC^{WT}$, in the presence or absence of the cross-linker BMOE, as indicated. The bifunctional, amine-reactive cross-linker DSP [dithiobis (succinimidyl propionate)] was added (0.2 mM for 30 min at 37 °C) to link the assembled pump components. Cross-linked complexes were analyzed by SDS/PAGE and immunoblotting with HlyA (intracellular toxin), HlyD (adaptor), HlyB (transporter), and TolC antiserum (adapted from ref. 1). The data confirm that asymmetric $TolC^{D374C}$, like $TolC^{WT}$, assembles into the tripartite pump (with transporter and adaptor) when induced by export substrate (intracellular toxin). (*D*) The asymmetric entrance does not function in an in vivo tripartite pump. HlyA export by the reconstituted $TolC^{D374C}$ pump with the inner-membrane transporter (HlyB) and adaptor (HlyD) was measured in the presence or absence of cross-linker BMOE. *E. coli* was grown to A_{600} 0.7 expressing $TolC^{WT}$ or $TolC^{D374C}$ and cell-free supernatant was collected by centrifugation and analyzed by immunoblotting with HlyA antiserum (adapted from ref. 1). The results show that when the pore constriction of $TolC^{D374C}$ is cross-linked into an asymmetric arrangement, toxin secretion by the substrate-engaged assembled tripartite pump is abolished. Conclusion: The results show that imposed asymmetry in the TolC pore constriction did not hinder assembly of the pump in response to engagement by the HlyA export substrate. However, the asymmetrical TolC entrance could not allow passage of substrate that was already engaged in the pump, i.e., it completely abolished the export function of TolC. The results provide no support for speculation that TolC opening is asymmetric.

1. Eswaran J, Hughes C, Koronakis V (2003) Locking TolC entrance helices to prevent protein translocation by the bacterial type I export apparatus. *J Mol Biol* 327:309–315.

Table S1. Data collection and refinement statistics for TolC open states

	$TolC^{RS}$	$TolC^{YFRS}$
Data collection		
Space group	$P\ 2_12_12_1$	$P\ 2_12_12_1$
Cell dimensions		
a, b, c (Å)	124.7, 135.2, 136.5	134.1, 135.5, 136.3
α, β, γ (°)	90.0, 90.0, 90.0	90.0, 90.0, 90.0
Lambda (Å)	0.9795	1.54
Unique reflections	51,195	104,232
Free *R* reflections (%)	2,611 (5.1)	5,282 (5.1)
Resolution range (last shell) (Å)	30.0–2.90 (3.08–2.90)	48.0–2.85 (3.00–2.85)
$I/\sigma I$ (last shell)	11.1 (3.8)	13.3 (3.3)
R_{merge} (last shell) (%)	12.5 (49.0)	10 (42.0)
Completeness (%)	98.9	93.9
Refinement		
Resolution (Å)	30.0–2.90	17.0–2.85
R_{work}/R_{free} (%)	25.8/30.1	27.3/30.9
Number of:		
Atoms	9,981	9,945
Residues	1,284	1,284
Waters	24	20
Wilson B factor	61.8	51.9
Refined protein B factor	59.6	62.8
Rms deviations		
Bond lengths (Å)	0.01	0.01
Bond angles (°)	1.2	1.2
Maximum-likelihood coordinate error (Å)	0.47	0.42
Ramachandran plot		
Most favored region (%)	1,191 (93.2)	1,189 (93.0)
Allowed region (%)	75 (5.9)	84 (6.6)
Outliers (%)	12 (0.9)	5 (0.4)